IOPscience iopscience.iop.org

Home Search Collections Journals About Contact us My IOPscience

Pressure-induced metallization in Mg_2Si

This content has been downloaded from IOPscience. Please scroll down to see the full text.

2017 J. Phys. D: Appl. Phys. 50 235304

(http://iopscience.iop.org/0022-3727/50/23/235304)

View the table of contents for this issue, or go to the journal homepage for more

Download details:

IP Address: 159.226.35.216
This content was downloaded on 19/06/2017 at 05:35

Please note that terms and conditions apply.

You may also be interested in:

Structural, vibrational, and electronic properties of BaReH9 under pressure
Eugene A Vinitsky, Takaki Muramatsu, Maddury Somayazulu et al.

Pressure-induced electronic topological transition in Sb2S3
Y A Sorb, V Rajaji, P S Malavi et al.

Atomic and electronic structures evolution of the narrow band gap semiconductor Ag2Se under high pressure
P Naumov, O Barkalov, H Mirhosseini et al.

Blue emitting organic semiconductors under high pressure: status and outlook
Matti Knaapila and Suchismita Guha

ScVO4 under non-hydrostatic compression: a new metastable polymorph
Alka B Garg, D Errandonea, P Rodríguez-Hernández et al.

Experimental and theoretical study of –Eu2(MoO4)3 under compression
C Guzmán-Afonso, S F León-Luis, J A Sans et al.

Effects of pressure and distortion on superconductivity in Tl2Ba2CaCu2O8+
Jian-Bo Zhang, Viktor V Struzhkin, Wenge Yang et al.

Magnetic-electronic properties of FeS and Fe7S8 studied by 57Fe Mössbauer and electrical measurements
S Takele and G R Hearne

An immutable array of TiO2 nanotubes to pressures over 30 GPa
Yanyan Zhang, Qinglin Wang, Junkai Zhang et al.

J. Phys. D: Appl. Phys. **50** (2017) 235304 (6pp) https://doi.org/10.1088/1361-6463/aa6e34

Pressure-induced metallization in Mg_2Si

J L Wang[1], S J Zhang[2], Y Liu[2], C Q Jin[2], N N Li[3], L J Zhang[1,3], Q J Liu[1], R Shen[1], Z He[1] and X R Liu[1]

[1] School of Physical Science and Technology, Key Laboratory of Advanced Technologies of Materials, Ministry of Education of China, Southwest Jiaotong University, Chengdu 610031, People's Republic of China
[2] Institute of Physics, Chinese Academy of Sciences, Beijing 100190, People's Republic of China
[3] Center for High Pressure Science and Technology Advanced Research (HPSTAR), Shanghai 201203, People's Republic of China

E-mail: xrliu@swjtu.edu.cn

Received 10 January 2017, revised 15 April 2017
Accepted for publication 20 April 2017
Published 19 May 2017

Abstract

Mg_2Si with narrow band gap has attracted increasing interest for its great potential applications. Theoretical calculations have predicted the metallization of Mg_2Si under high pressure. In this work, the electrical resistance and Raman spectrum measurements of semiconducting Mg_2Si were performed to investigate the metallization of Mg_2Si by using diamond anvil cells and strip opposite anvils. A discontinuous change of electrical resistance was found at around 10–13 GPa. Mg_2Si displays a semiconductive-like decreasing trend with increasing temperature before 10 GPa and a metallic-like increasing trend with increasing temperature after 13 GPa. The disappearance of Raman peaks above 9.7 GPa further supported the conclusion of metallization. These results suggest a semiconductor–metal transition at around 9.7 GPa in Mg_2Si, which is close to the theoretical predictive metallization at 6–8 GPa.

Keywords: metallization, high pressure, magnesium silicide

(Some figures may appear in colour only in the online journal)

1. Introduction

Magnesium silicide Mg_2Si has attracted considerable attention in recent years [1–6]. The interest is from its potential technological applications, low-cost production and nontoxicity. As a semiconductor with a narrow band gap of about 0.6 eV, Mg_2Si has been proposed to be infrared detectors working in the 1.2–2.0 μm wavelength range [7]. Mg_2Si and Mg_2Si-based alloys are good candidates for high-performance thermoelectric materials [8–11]. In addition, the hydrogenation property of Mg_2Si makes it a potential candidate for hydrogen storage [2]. Pressure has always been a good way to change electrical properties or structure of materials by extremely compressing the distance between atoms [12–14]. Morozova *et al* have reported the significant enhancement of thermoelectric properties of Al-based Mg_2Si under high pressure [11]. When investigating the effect of pressure on the thermoelectric properties of Mg_2Si, the knowledge of phase stability and phase transition under high pressure is very important [6, 10]. Available reports about Mg_2Si metallization under high pressure are largely inconsistent. Using energy dispersive x-ray diffraction, it was reported that Mg_2Si underwent a phase transition from the anti-fluorite to anti-cotunnite structure at 7.5 GPa, followed by a transition to the Ni_2In-type structure at 21.3 GPa [15]. Theoretical calculations suggested that both the anti-cotunnite type and Ni_2In type high-pressure phases are metallic [16]. Meanwhile, these calculations also predicted that the original semiconducting anti-fluorite type phase compressed to 6–8 GPa can exhibit a small finite density of states at the Femi level, thereby suggesting a metallization of this phase as a result of gradual band gap closing [6, 16, 17]. But experimental resistivity measurements under high pressure show that Mg_2Si underwent metallization transition at 22.2 GPa [18]. Moreover, Zhao *et al* reported that no structural phase transition in helium pressure-transmitting medium up to 14.7 GPa by synchrotron x-ray diffraction and predicted no metallization in Mg_2Si at least up to 22 GPa by calculation [10]. The inconsistency of

 © 2017 IOP Publishing Ltd Printed in the UK

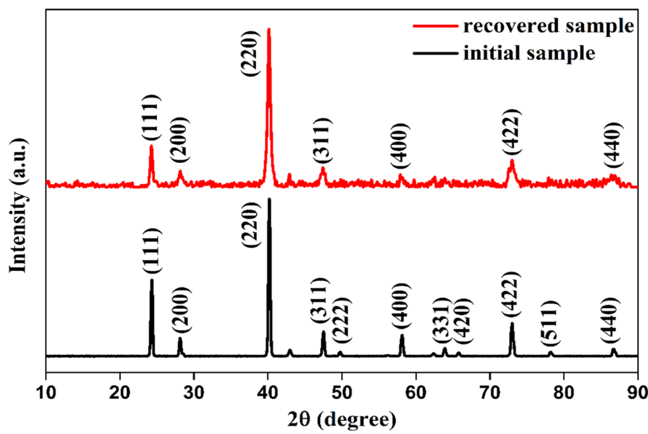

Figure 1. X-ray diffraction pattern of the initial Mg_2Si sample and the recovered Mg_2Si sample from high pressure.

experimental reports and theoretical predictions makes the metallization in Mg_2Si still controversial. Recently, Morozova *et al* reported Mg_2Si doped with 1 at.% of Al is metallized under moderate pressure between 5 and 12 GPa [11]. The excessive disparity in metallization pressure between pure Mg_2Si and Al-doped Mg_2Si draws more attention to this issue. A re-investigation therefore is very necessary in order to explore the metallization of pure Mg_2Si under high pressure.

2. Experimental section

The Mg_2Si powder (purity of 99.99%, Alfa Aesar Corporation) was checked to be anti-fluorite structure by x-ray diffraction (XRD, Panalytical X'pert, Cu K_α radiation) in figure 1. The electrical resistance measurement of Mg_2Si under high pressure was carried out in two ways. One way is continuously changing the pressure by using a setup of strip opposite anvils on hydraulic driven two-anvil press [19]. The picture of strip opposite anvils and schematic diagram of the sample assembly are shown in figure 2. The culet size of a strip opposite anvil is 20 mm × 5 mm and two pieces of pyrophyllite 23 mm × 5.5 mm × 0.55 mm were used as a gasket. A groove of about 8 mm × 1 mm × 0.2 mm was dug into one piece of pyrophyllite and Mg_2Si powder was filled in it. Four copper leg wires connect the sample to a constant direct current circuit and a recorder (GRAPHTEC GL900). The copper foil spacing is about 2 mm. The resistance value is calculated by Ohm's law. The constant current is 2 mA and 15 mA during compression and decompression respectively. The pressure was calibrated by Bi and ZnTe phase transitions [20–22]. The calibration curve is shown in figure 2(a). The pressure in the sample chamber is calculated from oil pressure according to the following calibration equation:

$$P(\text{GPa}) = -1.847\,14 + 2.006\,37 \times P_{\text{oil}}(\text{MPa}) - 0.090\,28 \times P_{\text{oil}}(\text{MPa})^2.$$

The other way is discontinuously changing the pressure by using diamond anvil cell (DAC). A traditional DAC with a culet of 300 μm was used to generate high pressure. The pressure was determined by the ruby fluorescence method at room temperature before and after each cooling down [23]. The pressure measured after each cooling down was used in the text. Combining with the Mag Lab system, we investigated the electronic transport properties under pressure at low temperatures. Mg_2Si was loaded into a hole in a pre-indented T301 stainless-steel gasket. The size of the Mg_2Si was about 60 μm × 60 μm × 5 μm. Cubic boron nitride was used as the insulating layer between the gasket and the electrodes. Sodium chloride was used as the transmitting medium. The four-probe method was adapted and the electrode leads were 18 μm-diameter gold wires. Raman scattering experiments of Mg_2Si powder under high pressure were performed up to 14.2 GPa on the back scattered Raman spectrometer (in-Via, Renishaw, 532 nm excitation wavelength). A T-301 stainless steel gasket was pre-indented and a 110 μm diameter hole was drilled at the center of the indentation by the laser. No pressure-transmitting was used. Pressure was determined by the shift of the ruby luminescence line [23].

3. Results and discussion

Mg_2Si is a rather soft material and its bulk modulus value was reported as $B_0 = 57$ GPa [15]. It was expected that its electronic band structure would be sensitive to stress and moderate high pressure should lead to drastic changes of resistivity [11]. Figure 3(a) shows the pressure dependence of electrical resistance at different temperatures by DAC. These pressure-dependent resistance curves showed a similar tendency. Upon compression, the resistance value of Mg_2Si decreased gradually. The drop of resistance was ascribed to the narrowing of band gap between the valence band and the conduction band under high pressure, which was also predicted by theoretical calculation [16, 17]. We noticed that the resistance difference under variation in temperature is larger at 0–2 GPa low fixed pressure than that at high fixed pressure. For semiconductor, the dependence of electrical resistivity on band gap and temperature can be close to exponential: $\rho \sim \exp\,[E_g/(2k_BT)]$, where k_B is Boltzmann's constant [11]. Increasing temperature can raise the number of electron carrier from the valence bands into the conduction bands and then lead to resistivity decline in Mg_2Si. Under pressure, although the band gap becomes narrower, carrier effective mass increases and the effect of temperature on carrier concentration is weakened [24]. Consequently, the temperature-induced variation in the resistance value of Mg_2Si becomes small with increasing pressure. Under high pressure, if there is a band gap closure and semiconductor Mg_2Si transforms to metallic phase, the temperature-induced variation in resistance value also has to be small for the pressure-induced increase if carrier effective mass is still dominant. Thus, further investigation about Mg_2Si metallization will help us to understand the temperature-dependent resistivity behavior under high pressure.

A logarithmic coordinate was used in figure 3(b), which has the advantage of displaying the resistance-pressure curve in the range of low resistance values. It was found that a discontinuous change of curve slope appeared at 10–13 GPa as the arrow shows. Whether this discontinuous change corresponds

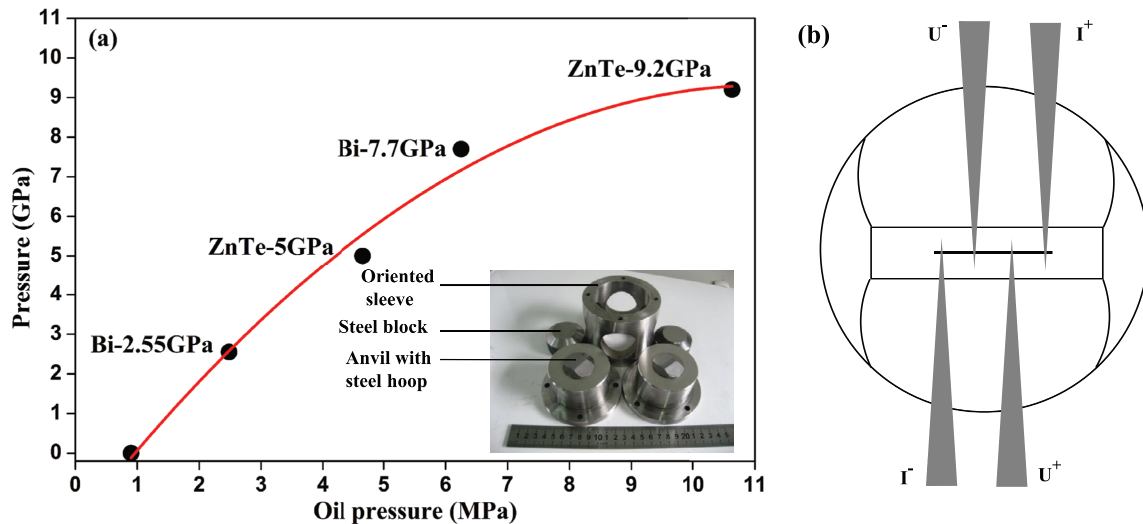

Figure 2. (a) Photo of strip anvils and the pressure calibration curve. (b) Schematic diagram of the sample assembly in a strip opposite anvil. The sample is put along the central line of the anvil. Four copper wires connect the sample to a constant current circuit (I^+ and I^- show the current flow) and a recorder (U^+ and U^- represent the recorded voltage of the sample).

to the metallization of Mg_2Si was then investigated through the temperature-dependent resistivity behavior. For metals, rising temperature will enhance the lattice vibrations and increase the possibility of electron scattering by phonons and then increase the resistivity [25]. For semiconductors, rising temperature can activate more charge carriers from the valence band into the conduction band and then decrease the resistivity [25]. Figure 3(c) displays the electrical resistance changing curves with increasing temperature under every pressure. As mentioned above, the resistance value of Mg_2Si is affected greatly by the variation in pressure. Considering that decreasing temperature usually causes the increase of pressure in DAC and in turn affects the resistance value, we selected the data of resistance value during increasing temperature at each selected pressure. As shown in figure 3(c), the electrical resistance of Mg_2Si displays a decreasing trend with the increasing temperature up to 10 GPa, which coincides with the behavior of semiconductor state. Above 13 GPa, the electrical resistance of Mg_2Si displays an increasing trend with the increasing temperature, which coincides with the behavior of metallic state. These results demonstrate that metallization of Mg_2Si probably occurred at 10–13 GPa.

Continuous variation curve of electrical resistance with pressure was measured on hydraulic driven two-anvil press. Figure 4(a) shows the pressure dependence of electrical resistance of Mg_2Si by the strip opposite anvils at room temperature. Upon compression, the resistance value of Mg_2Si dropped dramatically from the kilo ohm level, which corresponds to the compaction of loose Mg_2Si powders. Then one can see a smooth bend around 1–3 GPa. A similar phenomenon, i.e. the rapid drop at 0–1 GPa low pressure and gradual drop at 1–8 GPa and a smooth bend around 2–3 GPa in the electrical resistivity curve, were reported in Al-doped Mg_2Si by the quasi-four-probe method [11]. The smooth bend in the electrical resistivity curve was surmised to be related to some electrical crossovers or phase transitions [11]. The compaction of Mg_2Si powder, which was along with the densification of the gasket, usually caused the dramatic decrease of resistance value since air with higher resistivity is squeezed out. Thus, the smooth bend of the electrical resistance curve at around 2–3 GPa probably stemmed from the sample compaction instead of phase transition. In figure 4(b), after compaction, the resistance curve followed a linear trend with increasing pressure in logarithmic scale because the decrease in electrical resistance primarily comes from band gap narrowing under high pressure and the electrical resistivity is proportional to $\exp\,[E_g/(2k_BT)]$. We found that a change of resistance curve slope occurred at around 8.6 GPa. Above 8.6 GPa, the electrical resistance of Mg_2Si fell steeply with increasing pressure. Referring to theoretical predictions, the abrupt drop of electrical resistance was probably caused by the metallization of Mg_2Si. Theoretical calculation predicted a transition from anti-fluorite to metallic anti-cotunnite structure at around 8.38 GPa [6, 16]. The difference in metallization pressure between two experiments by DAC and automated strip opposite anvils probably stems from the different pressure measurement methods. Upon decompression, the resistance value of Mg_2Si increased gradually with decreasing pressure and finally returns to dozens of ohm as shown in figure 4(a). We measured the size of the recovered sample. In the case of ignoring the change of sample size during decompression, we calculated the electrical resistivity of the recovered Mg_2Si sample to be 0.25 $\Omega \cdot$ cm. The resistivity agrees well with that of original semiconductor Mg_2Si at ambient pressure in [18]. These results indicate that the pressure-induced band gap closing is reversible and the band gap broadens upon decompression. We also checked the structure of the recovered sample by XRD. As shown in figure 1, the recovered sample is anti-fluorite type phase. But compared with the initial sample, the crystallinity of the recovered sample became poor because its diffraction peaks broaden, intensity obviously declined and the weak peaks became almost invisible. We also found that

the crystallinity of the recovered sample became poorer after several compression cycles. The initial sample was prepared in suitable conditions for the crystal growth and so had good crystallinity. The recovered sample probably went through the recrystallization to anti-fluorite structure from anti-cotunnite structure during decompression. In such a recrystallization process, the pressure was varied and the crystal growth time was short. So it was difficult to form fine crystals and the diffraction peaks of the recovered sample seemed poor compared with that of the initial sample.

In this work, we investigated the evolution of the Raman spectrum of Mg_2Si under high pressure up to 14.2 GPa. The Mg_2Si in the anti-fluorite structure has two optical branches F_{2g} and F_{1u} in the vibrational dispersion curves [11, 26–30]. F_{2g} phonon mode is located at frequency range of 256.0–258.5 cm^{-1} and F_{1u} phonon mode frequency range 338.0–348.0 cm^{-1} [27–30]. Figure 5(a) shows the Raman spectra of Mg_2Si under selected pressures. The peak at around 256 cm^{-1} is the main peak and assigned to the F_{2g} phonon mode. The peak at around 341 cm^{-1} is assigned to the F_{1u} phonon mode. Figure 5(b) is the pressure dependence curve of the intensity of the two peaks. Figures 5(c) and (d) display the pressure dependence curves of the peak position and FWHM (full width at half maximum) of the two peaks, respectively. Upon compression, the intensity of the two peaks decreased persistently. It was ascribed to a gradual rising in the free carrier concentration [11]. For semiconductors, the band gap narrows under high pressure and the number of electron carriers from the valence bands into the conduction bands increases and then prevents the interaction between incident light and atoms. The profile of the Raman spectrum became very weak above 8.4 GPa. Finally, all peaks in the Raman spectrum disappeared at 9.7 GPa. The disappearance of the Raman vibration modes is ascribed to the metallization transition [31, 32]. The rising in the free carrier concentration after metallization prevents the laser light penetration into the sample [11]. Based on the Raman scattering data, we suggest that Mg_2Si metallized under moderate pressure 9.7 GPa. After decompression, the two peaks appeared again indicating the metallization is reversible. In figure 5(a), the Raman spectra of Mg_2Si above 3.2 GPa show different peak-like features. A shoulder peak appeared on the high wave number side of the main peak ~256 cm^{-1} as the arrow shows in figure 5(a). The split of the main peak caused a shift of peak position to high wave number at around 3.2 GPa in figure 3(c). Meanwhile, the FWHM of both peaks showed an abrupt increase at around 3.2 GPa in figure 5(d). Because the Raman spectroscopy measurements were done in non-hydrostatic conditions, the split and broadening of the Raman peaks above 3.2 GPa were probably driven by axial tension [33]. In figure 5(d), the increase of the FWHM with increasing pressure seemed stagnated at around 6.4 GPa and then increased above 7.7 GPa. The shift of the peak position of F_{1u} phonon mode showed a similar stagnation at around 6.4 GPa in figure 5(c). Although we noticed these discontinuous changes, it is hard to deduce possible phase transition in Mg_2Si before metallization in view of the increase of data inaccuracy. Above 5.2 GPa, the intensity of the Raman spectrum became further weakened. Consequently, the matching between the fitting peak and Raman peak profile decreased evidently due to the poor noise-signal ratio. From this point of view, Raman spectroscopy did not seem a suitable way to investigate the phase transition of Mg_2Si under high pressure because the rise in the free electron concentration caused the Raman spectrum to dramatically decline. But even so, we think that it is still necessary to investigate the possible phase transition before metallization in Mg_2Si in the future [6].

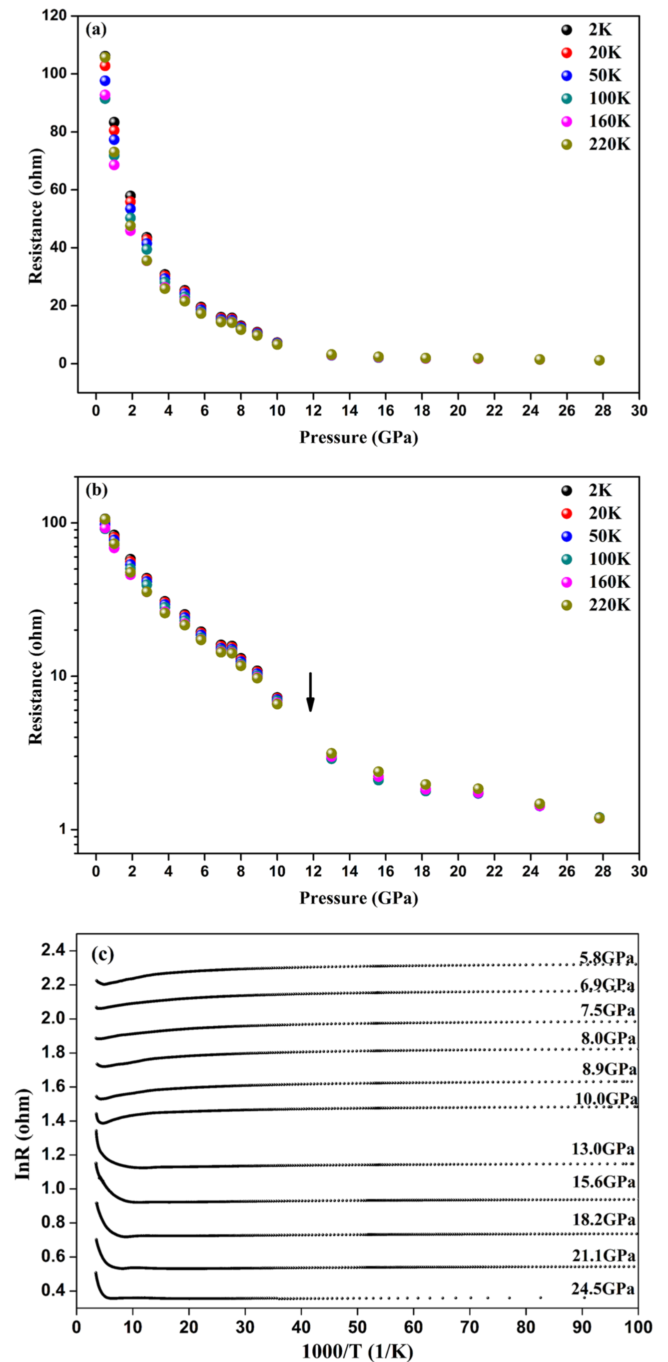

Figure 3. Pressure-dependent curves of electrical resistance of Mg_2Si at different temperatures by DAC under (a) linear coordinate and (b) logarithmic coordinate. (c) Temperature-dependent curves of electrical resistance of Mg_2Si under different pressures.

Available reports about structural phase transitions in Mg_2Si under high pressure are inconsistent. Theoretical calculation

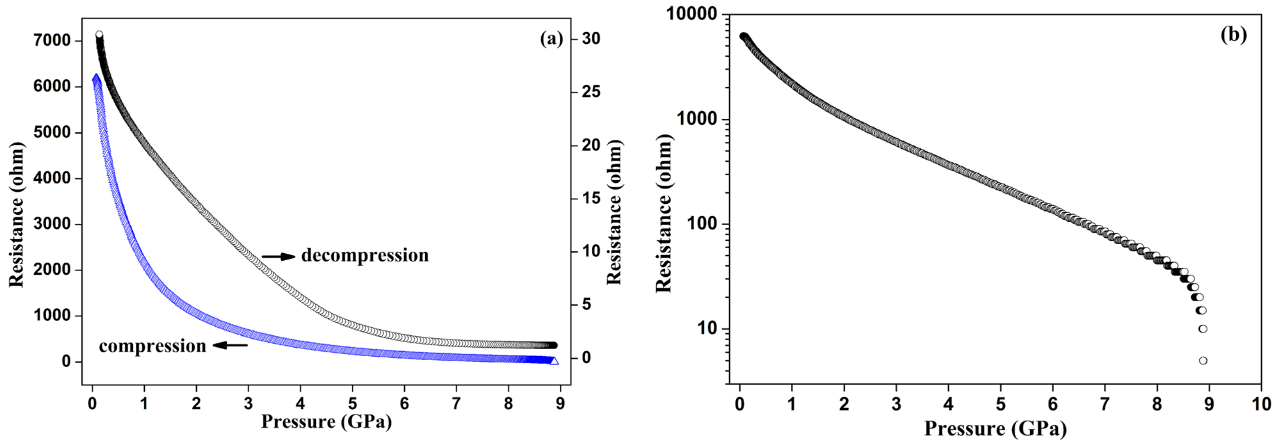

Figure 4. (a) Pressure dependence of electrical resistance of Mg_2Si at room temperature in the strip opposite anvils. (b) Electrical resistance-pressure curve in the logarithmic coordinate, which shows a dramatically drop of resistance at around 8.6 GPa.

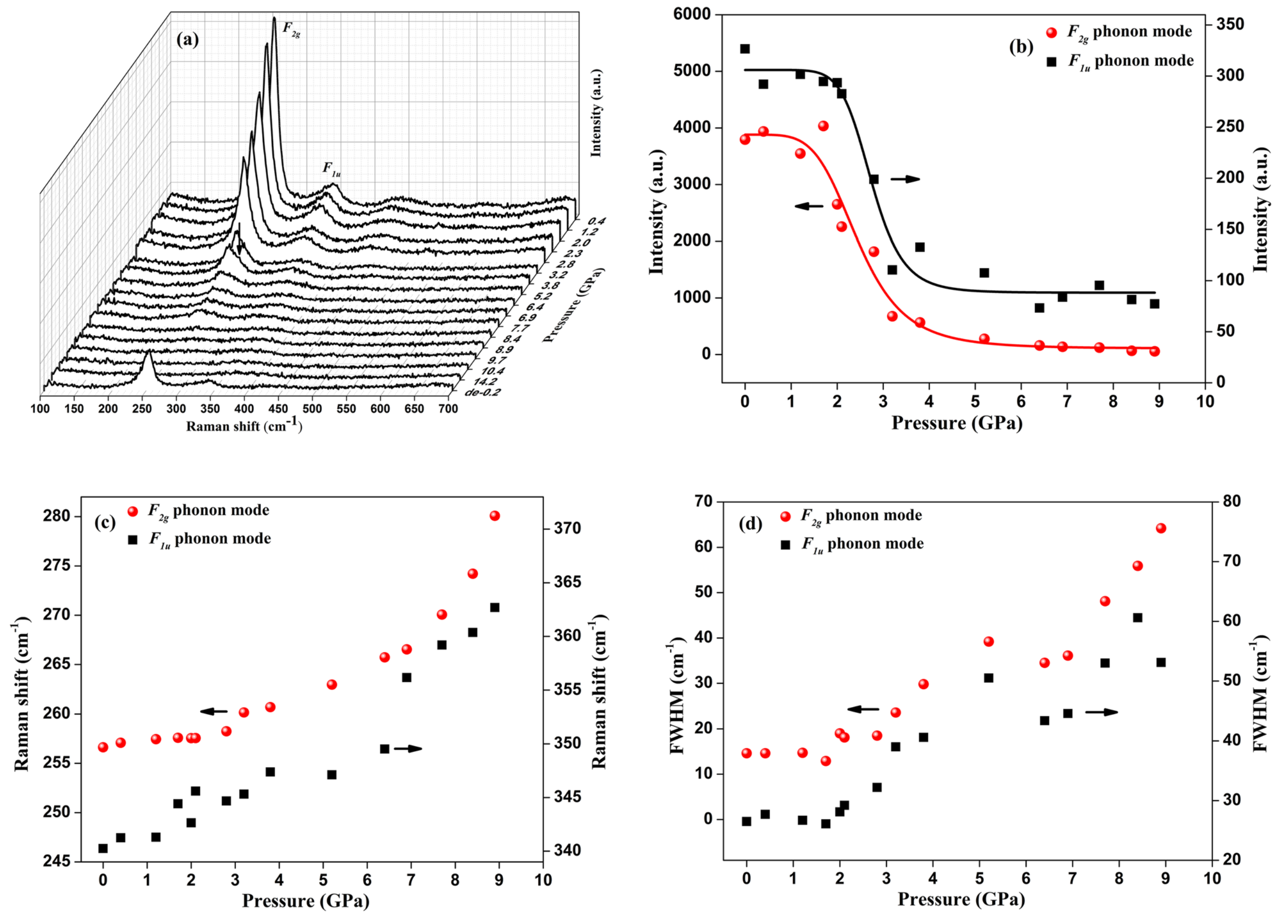

Figure 5. (a) Raman spectra of Mg_2Si under selected pressures. The Raman spectrum at 0.2 GPa during decompression is displayed. The pressure dependence of (b) peak intensity, (c) peak position, (d) FWHM of the F_{2g} and F_{1u} photon modes, which are located at 256 cm^{-1} and 341 cm^{-1} respectively at ambient pressure.

predicted that a transition from anti-fluorite to anti-cotunnite structure at around 8.38 GPa [6, 16]. Hao *et al* reported the transition from anti-fluorite to anti-cotunnite structure at around 7.5 GPa by energy dispersive synchrotron x-ray [15]. A variety of different structures, i.e. hexagonal and monoclinic structure have been reported at 6–12 GPa medium pressures [34, 35]. The studies of Zhao *et al* contradicted these earlier reports and suggested that no structural transition was observed in Mg_2Si up to 14.7 GPa by angle dispersive synchrotron x-ray diffraction [10]. The discrepancy between these diffraction measurements probably stem from different pressure-transmitting mediums being used [10, 15, 34]. The anti-fluorite crystal structure of Mg_2Si contains pores and when the atoms of pressure-transmitting medium enter the pores, this circumstance could affect the structural transition of Mg_2Si [10, 15, 34]. In this work, the metallization was

found at around 9.7 GPa by electrical resistance measurements and Raman spectroscopy. Referring to the theoretical prediction of phase transition from anti-fluorite to metallic anti-cotunnite structure at around 8.38 GPa, we speculated that the metallization of Mg_2Si at around 9.7 GPa was caused by the phase transition to anti-cotunnite structure under high pressure.

4. Conclusion

The metallization of Mg_2Si under high pressure was studied by the electrical resistance measurement and Raman spectroscopy. A discontinuous change of electrical resistance was observed at 10–13 GPa. Further investigations about the temperature-dependent resistivity behavior found that the Mg_2Si became metallic above 13 GPa. Raman analysis indicated that the Raman peaks disappeared above 9.7 GPa. It was ascribed to the fact that the rise in the free carrier concentration prevents the laser light penetration into the sample after metallization. These results suggest a semiconductor–metal transition at around 9.7 GPa in Mg_2Si, which is close to the theoretical predictions 6–8 GPa of metallization transition.

Acknowledgments

The corresponding author is grateful to Ming Zhang, Chunsheng Guo and Yuanzheng Chen for helpful discussion. We thank Wenge Yang and Li Lei for the aids in Raman scattering experiments. This work was financially supported by the National Natural Science Foundation of China (Grant No: U1530402 and 11304370) and Fundamental Research Funds for the Central Universities of China (Grant No: 2682014ZT31 and 2682016cx065).

References

[1] Zhou D, Liu J, Xu S and Peng P 2012 *Comput. Mater. Sci.* **51** 409–14
[2] Janot R, Cuevas F, Latroche M and Percheron-Guegan A 2006 *Intermetallics* **14** 163
[3] Bessas D, Simon R E, Friese K, Koza M and Hermann R P 2014 *J. Phys.: Condens. Matter* **26** 485401
[4] Chen S, Zhang X, Fan W, Yi T, Quach D V, Bux S, Meng Q, Kauzlarich S M and Munir Z A 2015 *J. Alloys Compd.* **625** 251–7
[5] Isoda Y, Tada S, Shioda N and Shinohara Y 2016 *J. Alloys Compd.* **656** 598–603
[6] Huan T D, Tuoc V N, Le N B, Minh N V and Woods L M 2016 *Phys. Rev.* B **93** 094109
[7] Udono H, Yamanaka Y, Uchikoshi M and Isshiki M 2013 *J. Phys. Chem. Solids* **74** 311–4
[8] Akasaka M, Iida T, Matsumoto A, Yamanaka K, Takanashi Y, Imai T and Hamada N 2008 *J. Appl. Phys.* **104** 013703
[9] Godlewska E M, Mars K, Drozdz P, Tchorz A and Ksiazek M 2016 *J. Alloys Compd.* **657** 755–64
[10] Zhao J, Liu Z, Gordon R A, Takarabe K, Reid J and Tes J S 2015 *J. Appl. Phys.* **118** 145902
[11] Morozova N V, Ovsyannikov S V, Korobeinikov I V, Karkin A E, Takarabe K, Mori Y, Nakamura S and Shchennikov V V 2014 *J. Appl. Phys.* **115** 213705
[12] Zhang S J, Wang X C, Sammynaiken R, Tse J S, Yang L X, Li Z, Liu Q Q, Desgreniers S, Yao Y, Liu H Z and Jin C Q 2009 *Phys. Rev.* B **80** 014506
[13] Zhang J L *et al* 2011 *Proc. Natl Acad. Sci. USA* **108** 24–8
[14] Li C, Zhao J, Hu Q, Liu Z, Yu Z and Yan H 2016 *J. Alloys Compd.* **688** 329–35
[15] Hao J, Zou B, Zhu P, Gao C, Li Y, Liu D, Wang K, Lei W, Cui Q and Zou G 2009 *Solid State Commun.* **149** 689–92
[16] Yu F, Sun J X, Yang W, Tian R G and Ji G F 2010 *Solid State Commun.* **150** 620–4
[17] Kalarasse F and Bennecer B 2008 *J. Phys. Chem. Solids* **69** 1775–81
[18] Ren W, Han Y, Liu C, Su N, Li Y, Ma B, Ma Y and Gao C 2012 *Solid State Commun.* **152** 440–2
[19] Tang F, Chen L, Liu X, Wang J, Zhang L and Hong S 2016 *Acta Phys. Sin.* **65** 100701
[20] Getting I C 1998 *Metrologia* **35** 119
[21] Ohtani A, Motobayashi M and Onodera A 1980 *Phys. Lett.* A **75** 435–7
[22] Ovsyannikov S V and Shchennikov V V 2004 *Solid State Commun.* **132** 333–6
[23] Mao H K, Xu J A and Bell P M 1986 *J. Geophys. Res.* **91** 4673–6
[24] Akselrod M M, Demchuk K M, Tsidilkovski I M, Broyda E L and Rodionov K P 1968 *Phys. Status Solidi* b **27** 249–54
[25] Eremets M I, Shimizu K, Kobayashi T C and Amaya K 1998 *Science* **281** 1333–5
[26] Buchenauer C J and Cardona M 1971 *Phys. Rev.* B **3** 2504
[27] Baleva M, Zlateva G, Atanassov A, Abrashev M and Goranova E 2005 *Phys. Rev.* B **72** 115330
[28] Whitten W B, Chung P L and Danielson G C 1965 *J. Phys. Chem. Solids* **26** 49–56
[29] Anastassakis E and Perry C H 1971 *Phys. Rev.* B **4** 1251
[30] Laughman L and Davis L W 1971 *Solid State Commun.* **9** 497–500
[31] Ponosov Y S, Ovsyannikov S V, Streltsov S V, Shchennikov V V and Syassen K 2009 *High Press. Res.* **29** 224–9
[32] Ovsyannikov S V, Gou H, Morozova N V, Tyagur I, Tyagur Y and Shchennikov V V 2013 *J. Appl. Phys.* **113** 013511
[33] Mohiuddin T M G *et al* 2009 *Phys. Rev.* B **79** 205433
[34] Zhu F, Wu X, Qin S and Liu J 2012 *Solid State Commun.* **152** 2160–4
[35] Cannon P and Conlin E T 1964 *Science* **145** 487–9